



Epoxy-Nanoceramic Composites for 5G Antennas

Hasanain B. Altaiebi*, Alaa A. Atiyah^{ORCID}, Saad B. H. Farid

Materials Engineering Dept., University of Technology-Iraq, Alsina'a street, 10066 Baghdad, Iraq.

*Corresponding author Email: mae.19.06@grad.uotechnology.edu.iq

HIGHLIGHTS

- Epoxy/ceramic composites were prepared using the solvent mixing method with four different volume fractions.
- The dielectric constant and loss tangent of composites were measured in the range of (4-8) GHz using Vector Network Analyzer (VNA)
- Epoxy composites with a 5 % volume fraction of $\text{Li}_6\text{Mg}_7\text{Ti}_3\text{O}_{16}$ are suitable for 5G antenna materials.

ARTICLE INFO

Handling editor: Akram R. Jabur

Keywords:

5G antenna
Inorganic nanoparticles
Microwave dielectric ceramics
Epoxy
Microwave dielectric properties

ABSTRACT

Epoxy-nanoceramic composites of BiVO_4 (BVO), LaNbO_4 (LNO), and $\text{Li}_6\text{Mg}_7\text{Ti}_3\text{O}_{16}$ (LMT) were prepared using the solvent mixing method. The ceramic nano-fillers volume fractions were (5, 8, 10, and 12%). X-ray diffraction (XRD) and Atomic Force Microscopy (AFM) were used to investigate the crystal structure and size distribution of nanoceramics, respectively. The dielectric constant and loss tangent were measured in the frequency range of (4-8) GHz. The measurement technique was the waveguide approach via a Vector Network analyzer (VNA). The effect of the volume fraction of ceramic fillers on the dielectric constant and loss tangent of the composites at 5.28 GHz (5G) was investigated. This work aims to design composite materials for 5G antennas of lower cost while maintaining the properties of 5G antennas. The results show that an optimum volume fraction of the ceramic filler brings the dielectric properties to their best value. However, epoxy composite with a 5% volume fraction of LMT shows good microwave dielectric properties (dielectric constant = 2.17 and loss tangent = 0.011) at 5.28 GHz. In addition, epoxy- LMT composite with an exceptionally low volume fraction of 5% provides a low-cost material for a 5G antenna. Another aspect of the cost reduction is the elimination of the costly and troublesome compaction and high-temperature sintering process. Furthermore, the epoxy composite overcomes the disadvantages of the high brittleness of the sintered all-ceramic products. As a result, epoxy composite with the 5% volume fraction of LMT is a potential candidate for 5G antenna materials.

1. Introduction

The fifth-generation (5G) network is a promising wireless communication technology that is recognized with three distinguishing features, namely high data transmission rate, reduced latency (delay time of signal transmission < 1 ms), and enormous device connectivity [1]. Internet of Things (IoT), mobile video streaming with download speeds exceeding 10 Gbit/s, autonomous vehicles, and smart traffic management, to name a few, have been enabled by 5G technology [2-4]. Antennas used in 5G technology require materials that satisfy a compact design, high gain, maximum capacity, and broad wireless spectrum [5-7].

Microwave Dielectric Ceramics (MWDCs) are among the candidate materials for a 5G antenna. The microwave dielectric properties of these ceramics are dielectric constant (ϵ_r), quality factor ($Q \times f$), and temperature coefficient of resonant frequency (τ_f). The values of these properties should be tuned to meet the criteria of a 5G antenna. For example, a high dielectric constant leads to a tiny antenna, but low dielectric constant results in a high data transfer rate. Signal integrity, selectivity, and energy transfer are all improved by a high-quality factor. The temperature stability of the active component is maintained by a near-zero temperature coefficient of resonant frequency [8-12]. However, despite their excellent dielectric properties, microwave dielectric ceramics have some drawbacks, including high brittleness, high sintering temperatures, complicated processing, and expensive cost, which represent crucial limitations on their uses [13, 14].

On the other hand, polymer-ceramic composites have also been developed to be used in microwave applications because they show enhanced dielectric, thermal, and mechanical features. In addition, the permittivity of these composites can be adjusted by varying the volume fraction of the filler material [15-17].

In this work, epoxy resin occupies a significant position among the available polymer materials due to its superior electrical, mechanical, thermal, and chemical characteristics, production simplicity, and geometrical design flexibility. Accordingly, the epoxy polymer is frequently utilized in electrical, electronic, and microelectronic applications [18, 19]. BiVO₄ (BVO), LaNbO₄ (LNO), and Li₆Mg₇Ti₃O₁₆ (LMT) nanopowders are chosen for the present paper due to their broad range of available dielectric constants. Additionally, these nanoceramics' large specific surface area causes strong interfacial bonding between the nanoceramic and the polymer matrix, enhancing the dielectric characteristics [20, 21].

This work aims to provide materials for a 5G antenna that have improved microwave dielectric properties (adequate dielectric constant and low loss tangent) while remaining inexpensive. That was via adopting epoxy matrix–nanofillers ceramics composites, which utilize much fewer expensive ceramics and inexpensive polymer casting compared with expensive powder processing and sintering.

2. Experimental

2.1 Materials

BiVO₄ (BVO), LaNbO₄ (LNO), and Li₆Mg₇Ti₃O₁₆ (LMT) nanoparticles with a purity of 99.9% were purchased from Nanoshel, India. Ethanol (Analytical grade) with a purity of 100% was supplied by Chem-Lab (Chem-Lab NV, Zedelgem, Belgium). Epoxy (EP) with a molecular weight of 393 was obtained from Sikadur®52 LP, Bahrain.

2.2 Specimen Preparation

The solvent mixing method was used to fabricate epoxy composites with volume fractions (5%, 8%, 10%, and 12%), as shown in Figure 1. First, the epoxy monomer was diluted with 5vol% ethanol to reduce viscosity and achieve easier casting. Next, the mix was stirred thoroughly (calm mixing) for 10 min using a glass rod. Then, the nanopowders were added to the mix and stirred for 10 min to form a homogeneous and stable suspension. At this step, the added ethanol also serves as a dispersing agent. Next, the curing agent was added by one part to two parts of the monomer. The mixture was stirred for 5 min. Finally, the mixture was poured into a silicon rubber mold, followed by a curing process at room temperature for 24h.

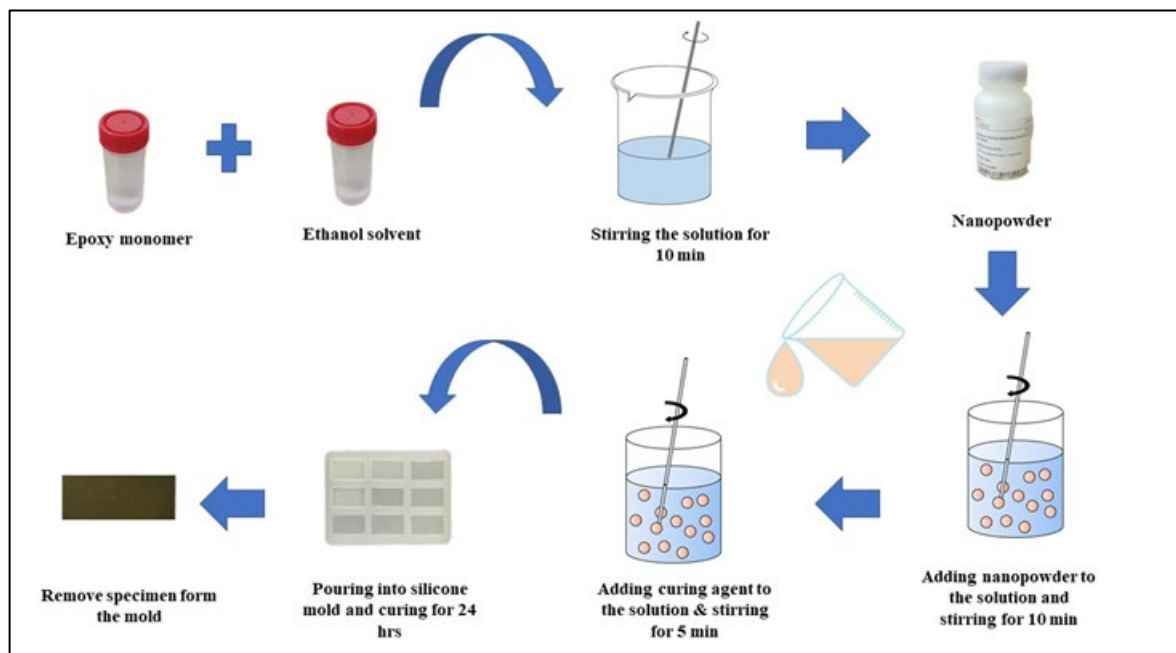


Figure 1: Schematic diagram representing the synthetic process of epoxy-nanoceramic composite

2.3 Materials Characterization

The XRD patterns of powder specimens were recorded by diffractometer (Shimadzu 6000) using wavelength (λ) 1.54 Å for CuK α radiation (40kV and 30mA). The scan range was from 10 to 80(deg). Step size and scan speed were 0.04 and 10 deg/min, respectively. In addition, the particle size characterization of the nanopowders was investigated using atomic force microscopy (NaioAFM, Nanosurf).

The permittivity of dielectrics is mathematically represented as a complex number:

$$\epsilon = \epsilon' - j\epsilon'' \tag{1}$$

The real component (ϵ') is the dielectric constant (the amount of electrical energy that can be stored in a material from an external electric field), while the imaginary component ($j\epsilon''$) is the dielectric loss (the measure of how much of electrical

energy loss due to an external electric field). The loss tangent is mathematically represented as a ratio of the imaginary component to the real component of permittivity [22-24].

$$\tan \delta = \varepsilon''/\varepsilon' \quad (2)$$

The permittivity and loss tangent of the specimens were measured with a thickness of 3mm using the waveguide method via the Anritsu MS4642A Vector Network Analyzer (VNA) in C-band (4-8GHz).

3. Results And Discussion

3.1 XRD and AFM Characterizations

3.1.1 XRD characterization

In the process of characterizing nanoparticles (NPs), X-ray diffraction (XRD) is one of the most widely employed methods. The elastic diffraction of X-rays on specimen atoms reveals details about lattice parameters, phase, crystalline grain size, and crystalline structure [25]. The XRD patterns of BiVO_4 , LaNbO_4 , and $\text{Li}_6\text{Mg}_7\text{Ti}_3\text{O}_{16}$ nanoparticles (NPs) display crystalline ceramics with sharp diffraction peaks, assigning a single phase for each. The XRD pattern of BiVO_4 , Figure 2, shows nine peaks at 18.666, 28.681, 30.972, 34.550, 39.765, 41.989, 45.547, 47.020, and 49.613 degrees, corresponding to the (hkl) Miller indices (101), (112), (004), (200), (114), (203), (214), (204), and (220), respectively. The peaks of BVO NPs represent a tetragonal structure. The diffraction peaks are indexed based on Powder Diffraction File (PDF-00-048-0744). The elementary cell parameters are as follows: ($a = b = 5.1940 \text{ \AA}$, $c = 11.5370 \text{ \AA}$, and $\alpha = \beta = \gamma = 90.0000^\circ$). The XRD pattern of LaNbO_4 , Figure 3, exhibits ten peaks at 28.174, 30.980, 33.440, 38.400, 39.380, 46.219, 48.061, 53.419, 56.600, and 58.260 degrees, corresponding to (112), (004), (200), (211), (114), (204), (220), (116), (312) and (224) planes, respectively. The diffracted peaks of LNO NPs correspond to the tetragonal structure. The diffraction peaks are labeled based on Powder Diffraction File (PDF-00-050-0919). The elementary cell parameters are as follows: ($a = b = 5.3500 \text{ \AA}$, $c = 11.5300 \text{ \AA}$, and $\alpha = \beta = \gamma = 90.0000^\circ$). The XRD pattern of $\text{Li}_6\text{Mg}_7\text{Ti}_3\text{O}_{16}$, Figure 4, displays fifteen peaks at 14.937, 18.322, 23.721, 26.015, 30.171, 33.835, 35.501, 43.122, 49.851, 57.071, 60.511, 62.653, 65.944, 74.166, and 79.134 planes, respectively. These can be indexed to the cubic structure of $\text{Li}_6\text{Mg}_7\text{Ti}_3\text{O}_{16}$ NPs. The diffraction peaks are indexed based on Powder Diffraction File (PDF-00-048-0263). The lattice parameters of the LMT powders are obtained: $a = b = c = 8.3774 \text{ \AA}$, and $\alpha = \beta = \gamma = 90.0000^\circ$.

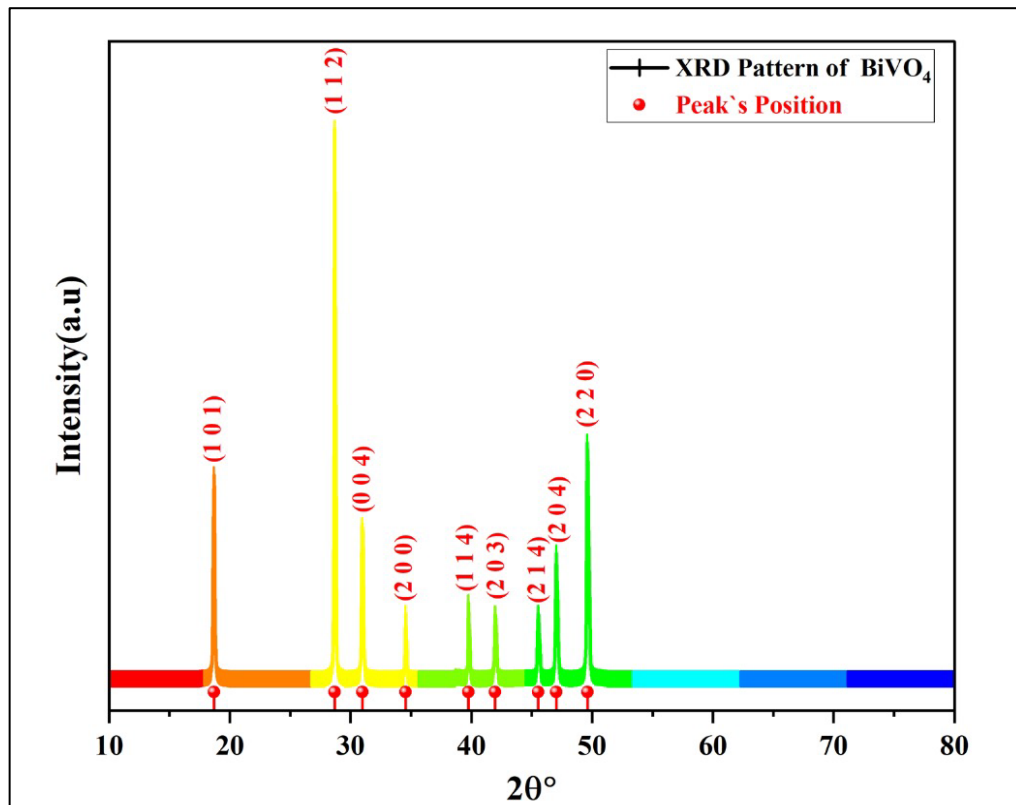


Figure 2: XRD patterns of BiVO_4 (PDF-00-048-0744)

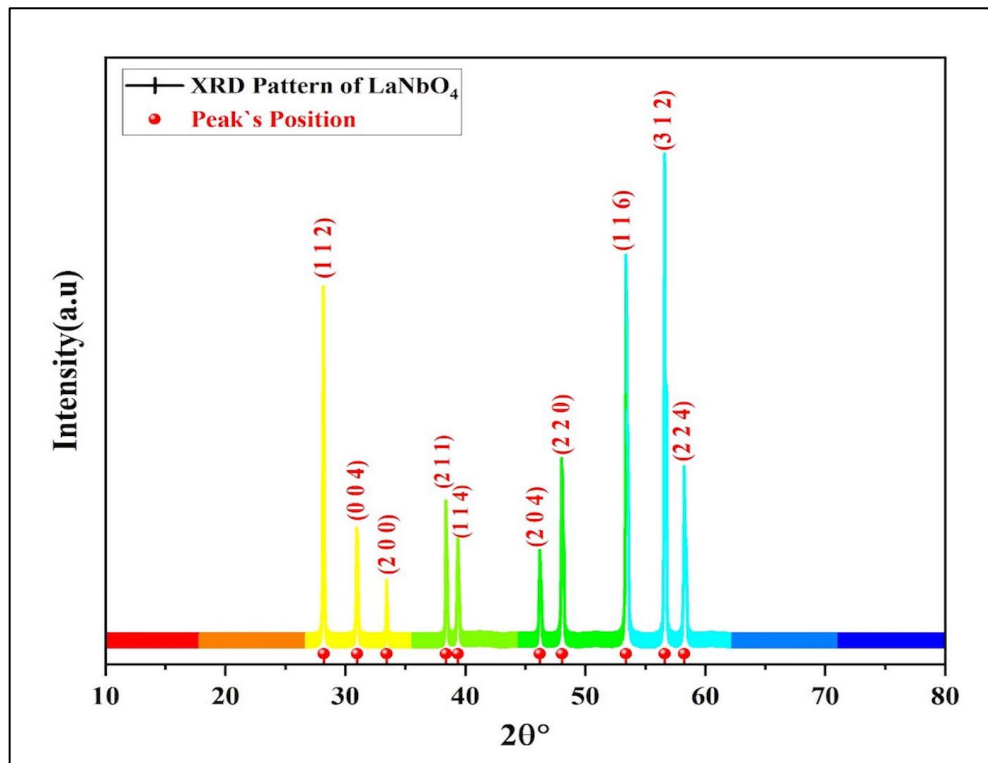


Figure 3: XRD patterns of LaNbO₄ (PDF-00-050-0919)

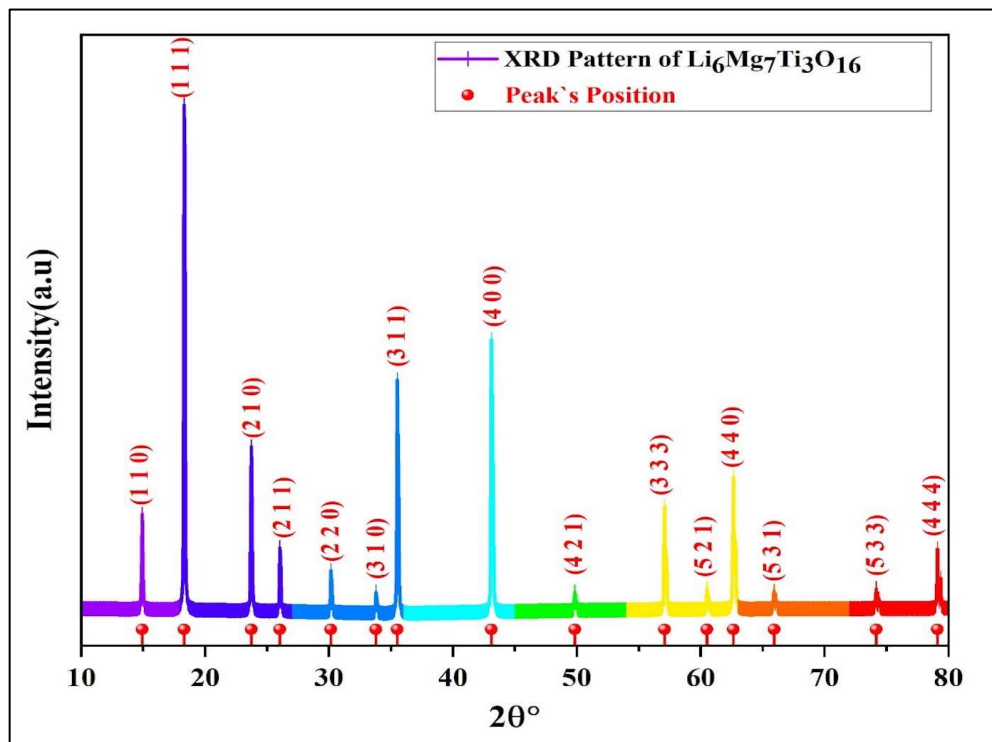


Figure 4: XRD patterns of Li₆Mg₇Ti₃O₁₆ (PDF-00-048-0263)

3.1.2 AFM characterization

Atomic force microscopy (AFM) is a key technology that provides high-resolution 3D images and statistical information such as shape, size, and surface roughness. It has the benefits over other methods since specimens do not need to be conductive, and high-pressure vacuum conditions are unnecessary [26]. Also, the particle size measurement obtained by AFM is compared with the laser particle size analyzer. The results show that both measurements are in good agreement and do not affect the outcomes of this paper. As can be seen in Figure 5, the BiVO₄, LaNbO₄, and Li₆Mg₇Ti₃O₁₆ nanoceramics have an average particle size of 57.26 nm, 18.16 nm, and 18.63 nm, respectively.

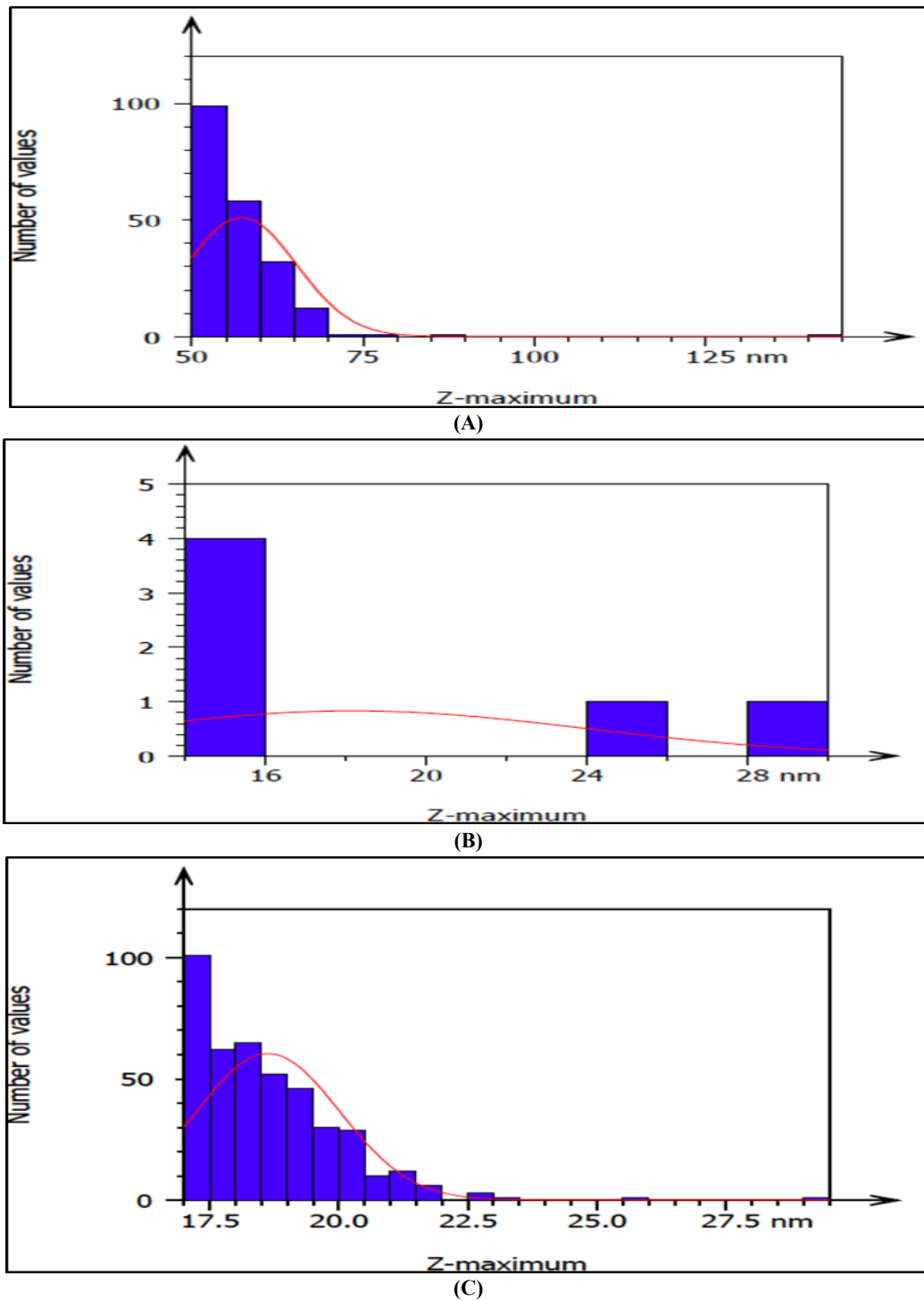


Figure 5: AFM measurements for the average particle size of the nanoceramics: (A) BiVO₄ = 57.26 nm, (B) LaNbO₄ = 18.16 nm, and (C) Li₆Mg₇Ti₃O₁₆ = 18.63 nm.

3.2 Electrical Characterization

According to Figure 6, the dielectric constant increases with the volume fraction of the ceramic nanofillers, i.e., the dielectric constant reflects the contribution of the ceramic nanofillers with direct proportionality. However, a drop in the dielectric constant for both EP-LNO and EP-LMT composites is noticed at a volume fraction of 10%. This drop can be attributed to the random internal scattering between defects within specimens [27]. LNO and LMT powders have an average particle size of nearly 18 nm, while it is around 57 nm for the BVO. Accordingly, the number of particles for the BVO is less than that for the other ceramics for the same volume fraction. This may indicate that the random internal scattering between defects is less for the EP-BVO composite. Hence, this effect is not noticed at 10 volume% and maybe exist at a higher (not examined) volume fraction. Figure 7 shows that the loss tangent has similar behavior to that of the dielectric constant, as compared with Figure 6. This may lead to the assumption that the loss tangent is merely proportional to the dielectric constant. These results are summarized in Table 1.

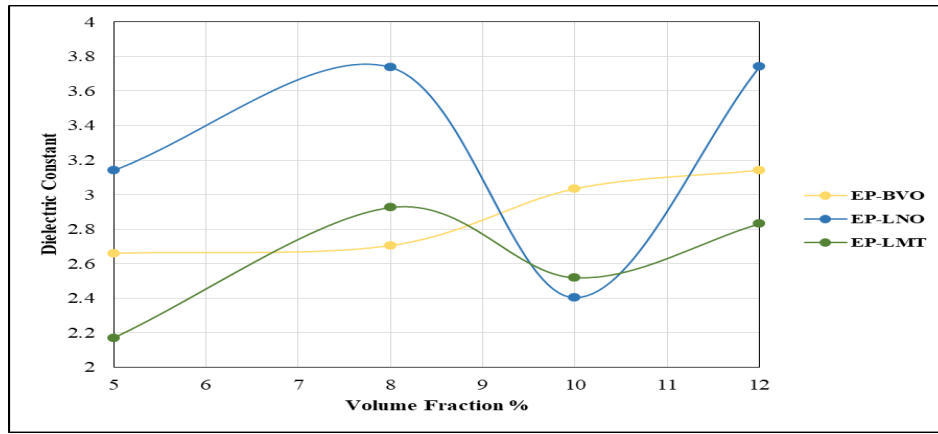


Figure 6: The dielectric constant of composites as a function of volume fraction of ceramic nanofillers, measured at room temperature and 5.28 GHz

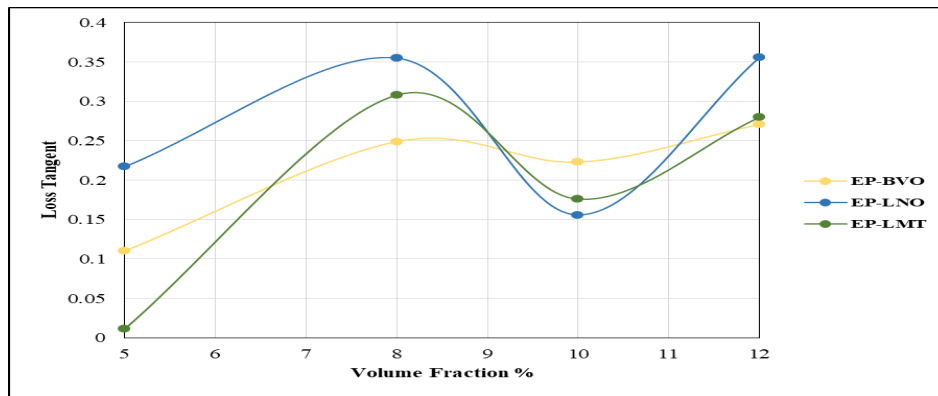


Figure 7: The loss tangent of composites as a function of the volume fraction of ceramic nanofillers, measured at room temperature and 5.28 GHz

Table 1: Summary of dielectric constant and loss tangent (at 5.28GHz) of epoxy composites as a function of filler volume fraction

EP composites	Dielectric constant as a function of the volume fraction of filler (%) @ 5.28 GHz				Loss tangent as a function of the volume fraction of filler (%) @ 5.28 GHz			
	5	8	10	12	5	8	10	12
EP-BVO	2.660	2.705	3.034	3.142	0.110	0.249	0.223	0.271
EP-LNO	3.140	3.738	2.403	3.742	0.217	0.355	0.156	0.356
EP-LMT	2.169	2.925	2.518	2.831	0.011	0.308	0.176	0.280

Table 2: Comparison of microwave dielectric properties with other materials

Material	Frequency	Dielectric Constant	Loss Tangent	References
FR-406	5GHz	3.92	0.017	[28]
RT/Duroid 5870	1MHz-10GHz	2.33±0.02	0.0012	[29]
RT/Duroid 5880	1MHz-10GHz	2.20±0.02	0.0009	[29]
Polytetrafluoroethylene- TeO ₂ (60% volume fraction)	7GHz	5.4	0.006	[30]
Butyl rubber- SiO ₂ (26% volume fraction)	5GHz	2.79	0.0039	[31]
Polydimethylsiloxane- BaFe ₁₂ O ₁₉ (30% volume fraction)	35GHz	~5	0.045	[32]
EP-LMT (5% volume fraction)	5.28GHz	2.169	0.011	Present work

Table 2 shows a comparison of microwave dielectric properties with other materials. Based on this table, the microwave dielectric properties of epoxy composites with a 5% volume fraction of LMT have the advantages of both low dielectric constant (RT/Duroid 5870 & RT/Duroid 5880) and the low loss tangent of FR-406. In addition, the present work's ceramic volume fraction is very low compared to ref [30]. On the other hand, compared to ref [31], the present work demonstrates a smaller volume fraction while maintaining an approximately similar value for the dielectric constant. Moreover, the volume

fraction and loss tangent in the present work are smaller than in ref [32]. Accordingly, epoxy composite with a 5% volume fraction of LMT is a good alternative material for 5G antennas.

4. Conclusions

Three epoxy/ceramic composites were prepared using solvent mixing method with four different volume fractions. The ceramic nanofillers include BiVO₄, LaNbO₄, and Li₆Mg₇Ti₃O₁₆. The dielectric properties of these composites were studied as a function of ceramic loading at 5.28 GHz. Low-cost composite materials with very low volume fractions are achieved by incorporating nanosized fillers in a polymer matrix. The composite approach also avoids the drawbacks of producing microwave dielectric ceramics, such as high brittleness, high processing temperatures, and expensive milling. The composites with a 5 % volume fraction of Li₆Mg₇Ti₃O₁₆ are suitable for 5G antenna materials due to the moderate dielectric constant and low loss tangent.

Author contribution

All authors contributed equally to this work.

Funding

This research received no specific grant from any funding agency in the public, commercial, or not-for-profit sectors.

Data Availability Statement

Not applicable.

Conflicts of Interest

The authors of the current work do not have a conflict of interest

References

- [1] H. Hao, D. Hui, D. Lau, Material advancement in technological development for the 5G wireless communications, *Nanotechnol. Rev.*, 9 (2020) 683-699. <https://doi.org/10.1515/ntrev-2020-0054>
- [2] A.C. Sodr , I.F. da Costa, R.A. dos Santos, H.R.D. Filgueiras, D.H. Spadoti, Waveguide-Based Antenna Arrays for 5G Networks, *Int. J. Antennas Propag.*, 2018 (2018) 1-10. <https://doi.org/10.1155/2018/5472045>
- [3] H. Al-Saif, M. Usman, M.T. Chughtai, J. Nasir, Compact Ultra-Wide Band MIMO Antenna System for Lower 5G Bands, *Wireless Commun. Mobile Comput.*, 2018 (2018) 1-6. <https://doi.org/10.1155/2018/2396873>
- [4] D.Y.C. Lie, J.C. Mayeda, Y. Li, J. Lopez, A Review of 5G Power Amplifier Design at cm-Wave and mm-Wave Frequencies, *Wireless Commun. Mobile Comput.*, 2018 (2018) 1-16. <https://doi.org/10.1155/2018/6793814>
- [5] K. Khamoushi, Characterization and Dielectric Properties of Microwave Rare Earth Ceramics Materials for Telecommunications, arXiv preprint arXiv:1509.04445, (2015). <https://doi.org/10.48550/arXiv.1509.04445>
- [6] M. Yang, Y. Sun, F. Li, A Compact Wideband Printed Antenna for 4G/5G/WLAN Wireless Applications, *Int. J. Antennas Propag.*, 2019 (2019) 1-9. <https://doi.org/10.1155/2019/3209840>
- [7] S. N.H. Sa'don, M.H. Jamaluddin, M.R. Kamarudin, F. Ahmad, Y. Yamada, K. Kamardin, I.H. Idris, Analysis of Graphene Antenna Properties for 5G Applications, *Sensors (Basel)*, 19 (2019). <https://doi.org/10.3390/s19224835>
- [8] Y. Ji, K. Song, S. Zhang, Z. Lu, G. Wang, L. Li, D. Zhou, D. Wang, I.M. Reaney, Cold sintered, temperature-stable CaSnSiO₅-K₂MoO₄ composite microwave ceramics and its prototype microstrip patch antenna, *J. Eur. Ceram. Soc.*, 41 (2021) 424-429. <https://doi.org/10.1016/j.jeurceramsoc.2020.08.053>
- [9] S. Wang, W. Luo, L. Li, M. Du, J. Qiao, Improved tri-layer microwave dielectric ceramic for 5 G applications, *J. Eur. Ceram. Soc.*, 41 (2021) 418-423. <https://doi.org/10.1016/j.jeurceramsoc.2020.09.008>
- [10] L. Zhang, J. Zhang, Z. Yue, L. Li, New three-phase polymer-ceramic composite materials for miniaturized microwave antennas, *AIP Adv.*, 6 (2016) 095319-1–095319-9. <https://doi.org/10.1063/1.4964150>
- [11] D. Zhou, L.-X. Pang, D.-W. Wang, Z.-M. Qi, I.M. Reaney, High Quality Factor, Ultralow Sintering Temperature Li₆B₄O₉ Microwave Dielectric Ceramics with Ultralow Density for Antenna Substrates, *ACS Sustainable Chem. Eng.*, 6 (2018) 11138-11143. <https://doi.org/10.1021/acssuschemeng.8b02755>
- [12] W. A.W. Muhamad, R. Ngah, M.F. Jamlos, P.J. Soh, M.A. Jamlos, H. Lago, Antenna array bandwidth enhancement using polymeric nanocomposite substrate, *Appl. Phys. A*, 122 (2016). <https://doi.org/10.1007/s00339-016-9887-z>
- [13] L. Zhang, J. Zhang, Z. Yue, L. Li, Thermally stable polymer–ceramic composites for microwave antenna applications, *J. Adv. Ceram.*, 5 (2016) 269-276. <https://doi.org/10.1007/s40145-016-0199-8>

- [14] M. P.F. Graça, K.D.A. Sabóia, F. Amaral, L.C. Costa, Microwave Dielectric Properties of CCTO/PVA Composites, *Adv. Mater. Sci. Eng.*, 2018 (2018) 1-7. <https://doi.org/10.1155/2018/6067519>
- [15] Z. H. Jiang, Y. Yuan, Microwave dielectric properties of SrAl₂Si₂O₈ filled Polytetrafluoroethylene composites, *IOP Conf. Ser.: Mater. Sci. Eng.*, 479,2019. <https://doi.org/10.1088/1757-899x/479/1/012090>
- [16] S. K. Yoon, H.G. Lee, W.S. Lee, E.S. Kim, Dielectric properties of ZnNb₂O₆/epoxy composites, *J. Electroceram.*, 30 (2013) 93-97. <https://doi.org/10.1007/s10832-012-9737-0>
- [17] S. Dash, R.N.P. Choudhary, A. Kumar, M.N. Goswami, Enhanced dielectric properties and theoretical modeling of PVDF–ceramic composites, *J. Mater. Sci. Mater. Electron.*, 30 (2019) 19309-19318. <https://doi.org/10.1007/s10854-019-02291-z>
- [18] N. Hasan, N.S.M. Hussain, A.A.M. Faudzi, S.M. Shaharum, N.A.T. Yusof, N.H. Noordin, N.A.A. Mohtadzar, M.S.A. Karim, Cured epoxy resin dielectric characterization based on accurate waveguide technique, *AIP Conference Proceedings*, 2129, 2019, 020080. <https://doi.org/10.1063/1.5118088>
- [19] S. M. Seng, K.Y. You, F. Esa, M.Z.H. Mayzan, Dielectric and Magnetic Properties of Epoxy with Dispersed Iron Phosphate Glass Particles by Microwave Measurement, *J. Microw. Optoelectron. Electromagn. Appl.*, 19 (2020) 165-176. <https://doi.org/10.1590/2179-10742020v19i2824>
- [20] T. H. Lin, P.M. Raj, A. Watanabe, V. Sundaram, R. Tummala, M.M. Tentzeris, Nanostructured miniaturized artificial magnetic conductors (AMC) for high-performance antennas in 5G, IoT, and smart skin applications, 2017 IEEE 17th International Conference on Nanotechnology (IEEE-NANO), Pittsburgh, PA, USA, 2017, 911-915. <https://doi.org/10.1109/NANO.2017.8117483>
- [21] Oliveira, A.D. d. Polymer Nanocomposites with Different Types of Nanofiller, *Nanocomposites - Recent Evolutions*, 2019. <https://doi.org/10.5772/intechopen.81329>
- [22] G. Shimoga, S.-Y. Kim, High-k Polymer Nanocomposite Materials for Technological Applications, *Appl. Sci.* 10 (2020). <https://doi.org/10.3390/app10124249>
- [23] L. Wang, J. Yang, W. Cheng, J. Zou, D. Zhao, Progress on Polymer Composites With Low Dielectric Constant and Low Dielectric Loss for High-Frequency Signal Transmission, *Front. Mater.*, 8 (2021). <https://doi.org/10.3389/fmats.2021.774843>
- [24] X. Huang, B. Sun, Y. Zhu, S. Li, P. Jiang, High-k polymer nanocomposites with 1D filler for dielectric and energy storage applications, *Prog. Mater. Sci.*, 100 (2019) 187-225. <https://doi.org/10.1016/j.pmatsci.2018.10.003>
- [25] S. Mourdikoudis, R.M. Pallares, N.T. Thanh, Characterization techniques for nanoparticles: comparison and complementarity upon studying nanoparticle properties, *Nanoscale*, 10 (2018) 12871-12934. <https://doi.org/10.1039/C8NR02278J>
- [26] M. Govindarajan, G. Benelli, A Facile One-Pot Synthesis of Eco-Friendly Nanoparticles Using Carissa carandas: Ovicidal and Larvicidal Potential on Malaria, Dengue and Filariasis Mosquito Vectors, *J. Clus. Sci.*, 28 (2016) 15-36. <https://doi.org/10.1007/s10876-016-1035-6>
- [27] H.Y. Yao, Y.W. Lin, T.H. Chang, Dielectric Properties of BaTiO₃-Epoxy Nanocomposites in the Microwave Regime, *Polymers*, 13 (2021) 1391. <https://doi.org/10.3390/polym13091391>
- [28] M. Zhang, P. Xu, H. Peng, F. Qin, A rational design of core-shell-satellite structured BaTiO₃ fillers for epoxy-based composites with enhanced microwave dielectric constant and low loss, *Compos. B. Eng.*, 215 (2021) 108764. <https://doi.org/10.1016/j.compositesb.2021.108764>
- [29] N. Hasan, N. H. Noordin, M.S.A. Karim, M.R.M. Rejab, Q.J. Ma, Dielectric properties of epoxy–barium titanate composite for 5 GHz microstrip antenna design, *SN Appl. Sci.*, 2 (2019). <https://doi.org/10.1007/s42452-019-1801-9>
- [30] G. Subodh, M. Joseph, P. Mohanan, M.T. Sebastian, Low Dielectric Loss Polytetrafluoroethylene/TeO₂Polymer Ceramic Composites, *J. Am. Ceram. Soc.*, 90 (2007) 3507-3511. <https://doi.org/10.1111/j.1551-2916.2007.01914.x>
- [31] J. Chameswary, M.T. Sebastian, Effect of Ba(Zn_{1/3}Ta_{2/3})O₃ and SiO₂ ceramic fillers on the microwave dielectric properties of butyl rubber composites, *J. Mater. Sci.: Mater. Electron.*, 24 (2013) 4351-4360. <https://doi.org/10.1007/s10854-013-1410-0>
- [32] R. Bowrothu, H.-I. Kim, C.S. Smith, D.P. Arnold, Y.-K. Yoon, 35-GHz Barium Hexaferrite/PDMS Composite-Based Millimeter-Wave Circulators for 5G Applications, *IEEE. Trans. Microw. Theory. Tech.*, 68 (2020) 5065-5071. <https://dx.doi.org/10.1109/tmtt.2020.3022556>